applied sciences

MDPI

Article

Thermal Grading Strategies in Multi-Reactor $LaNi_5$ Metal Hydride Systems: Energy, Exergy, and Pressure Amplification Analysis

Nesrin İlgin Beyazit

Department of Mechanical Engineering, Faculty of Engineering, Dicle University, 21280 Diyarbakır, Türkiye; nesrin.ilgin@dicle.edu.tr

Abstract

Metal hydride-based hydrogen storage and compression systems provide a safe, efficient approach to hydrogen transfer; however, the effect of temperature distribution direction on the overall performance of multi-reactor systems remains poorly understood. This study compares a $LaNi_5$-based single-reactor system with three multi-reactor thermal cascading strategies: increasing-temperature cascading, decreasing-temperature cascading, and isothermal operation. The study evaluated thermodynamic, exergy, and thermo-flow characteristics while maintaining a constant total metal hydride inventory of 3 kg. The results show that increasing temperature cascading delivered the strongest pressure-amplification performance, achieving a progressive pressure rise across the reactor sequence and an equilibrium-pressure amplification ratio of 4.48. In contrast, decreasing temperature cascading produced an unfavorable pressure distribution and reduced the equilibrium-pressure amplification ratio to 0.22. Although the increasing-temperature configuration did not achieve the highest exergy efficiency, it provided the greatest pressure amplification capability and the highest overall exergy–pressure performance index. Thermo-flow analysis further indicated improved heat-transfer organization and more stable hydrogen transport under directional temperature gradients. The findings demonstrate that temperature distribution direction is a key design parameter for enhancing the performance of multi-reactor metal hydride systems.

Keywords: metal hydride; hydrogen storage; hydrogen compression; multi-reactor system; thermal cascading; exergy analysis; thermo-flow behavior; $LaNi_5$

Check for updates

Academic Editor: Luisa F. Cabeza

Received: 24 June 2026
Revised: 22 September 2026
Accepted: 25 September 2026
Published: 27 September 2026

Copyright: © 2026 by the author. Licensee MDPI, Basel, Switzerland. This article is an open access article distributed under the terms and conditions of the Creative Commons Attribution (CC BY) license.

1. Introduction

Metal hydride (MH)-based hydrogen storage and compression systems have become an important research area in sustainable hydrogen technologies because of their high volumetric energy density, safe operating conditions, and low need for mechanically moving components [1–3]. In particular, $LaNi_5$-, TiFe-, and MgH_2-based alloys are widely used in hydrogen storage and hydrogen transfer applications because of their stable thermodynamic behavior and favorable hydrogen absorption/desorption characteristics [1,4–6]. Nevertheless, the performance of metal hydride systems depends not only on alloy properties but also directly on the effectiveness of heat and mass transfer mechanisms within the reactor [5,7,8].

In metal hydride reactors, absorption is exothermic, whereas desorption is endothermic [1,9]. Consequently, insufficient management of the heat released during absorption

or the heat supplied during desorption significantly limits reaction kinetics and hydrogen transfer performance [10,11]. To improve heat-transfer characteristics, numerous studies have investigated multi-tubular reactor configurations, finned geometries, phase change material (PCM)-assisted systems, and various heat exchanger designs [7,8,10–14]. Pandey et al. [11] demonstrated that optimized fin arrangements could significantly reduce absorption time. Similarly, Ye et al. [15] and Atalmis et al. [16] reported that enhanced thermal conductivity improves reaction kinetics and hydrogen storage performance.

Recent studies have shown that improvements at the single-reactor level alone are insufficient and that thermal integration plays a critical role in multi-stage metal hydride systems [17–19]. In this context, energy–exergy analyses and parametric evaluations have become important tools for optimizing system performance [19–21]. In particular, multi-stage metal hydride compressor systems have attracted considerable attention because they can produce high-pressure hydrogen using low-grade waste heat sources [1,17,18,22]. Parida et al. [18] demonstrated that a three-stage metal hydride compressor system could achieve pressure levels of approximately 300 bar. However, many existing studies have focused primarily on single-reactor performance or solely on pressure amplification. In contrast, the effects of different thermal cascading strategies on energy, exergy, and thermo-flow behavior remain limited [7,11]. Beyond stationary hydrogen storage and compression applications, reliable hydrogen storage and delivery at suitable pressure levels are also important for sustainable transportation technologies based on fuel-cell propulsion. In particular, hydrogen fuel-cell buses require coordinated integration of hydrogen storage, supply, and electric propulsion subsystems to operate efficiently and reliably. Recent studies on autonomous hydrogen fuel-cell buses have further emphasized the technological relevance of hydrogen-based propulsion systems for sustainable public transport and long-range mobility [23]. Accordingly, improvements in thermally driven hydrogen storage and pressure-management technologies may also contribute to the broader development of hydrogen-based transportation systems.

Under desorption conditions, increasing the temperature along the reactors raises the equilibrium pressure according to the Van't Hoff relationship, creating a natural pressure-amplification mechanism within the system [6,9,17,24]. In contrast, decreasing temperature cascading weakens the thermodynamic driving force, whereas under isothermal conditions no significant pressure gradient is formed between the reactors. This behavior indicates that not only the temperature level but also the temperature distribution pattern is a fundamental thermodynamic design parameter governing hydrogen-transfer mechanisms, pressure-propagation behavior, and overall system performance in multi-reactor metal hydride systems.

Previous studies on multi-stage metal hydride hydrogen compression have primarily focused on alloy selection, reactor geometry, heat-transfer enhancement, stage operating windows, or the overall pressure lift obtained between prescribed low- and high-temperature conditions. In contrast, this study isolates the direction of inter-reactor temperature grading as the principal comparative variable. Using the same $LaNi_5$ inventory, the same set of reactor temperatures, and a common thermodynamic evaluation basis, the study compares increasing, decreasing, and isothermal temperature distributions in terms of equilibrium-pressure ordering, thermal-exergy characteristics, and reduced-order thermo-flow behavior. Thus, the novelty of the present work lies not in proposing a new compressor cycle, but in systematically examining how reversing the thermal-grading direction modifies the equilibrium-pressure amplification tendency and associated thermal behavior within an otherwise consistent multi-reactor framework. The single-reactor and thermally graded multi-reactor configurations considered in this study are schematically illustrated in Figure 1.

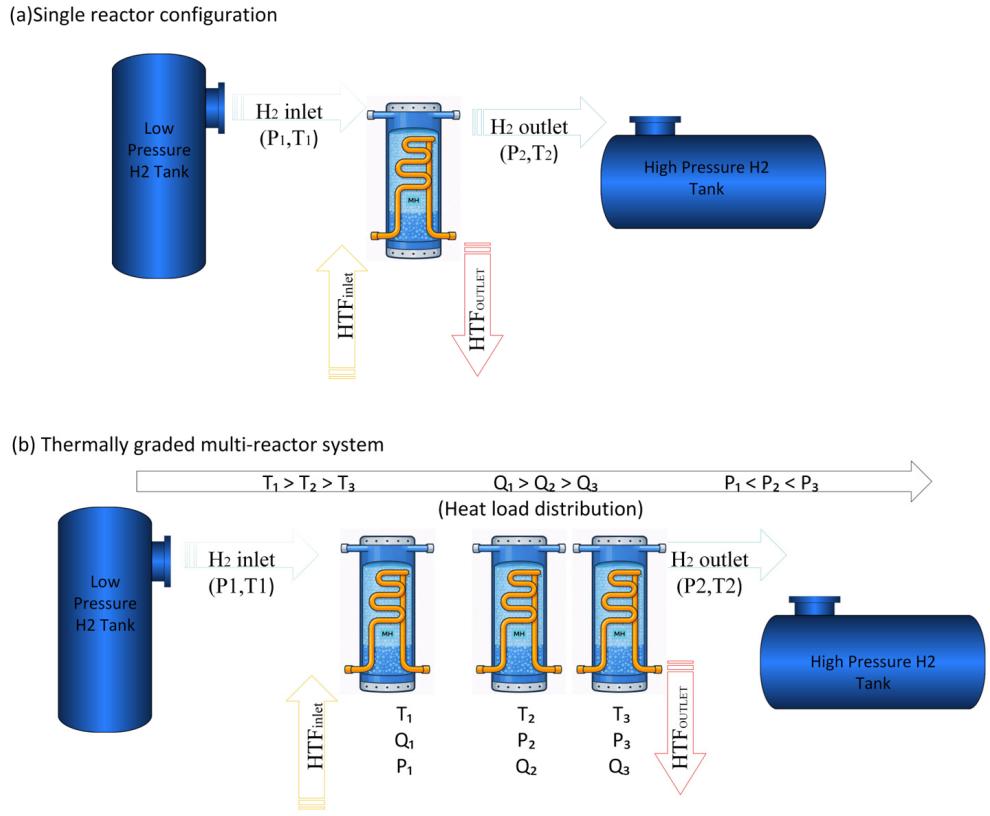


Figure 1. Schematic representation of (**a**) the single-reactor configuration and (**b**) the thermally graded multi-reactor configuration, illustrated for the increasing-temperature case (T1 < T2 < T3 and P1 < P2 < P3). The decreasing-temperature and isothermal cases use the same reactor arrangement with reversed and equal temperature assignments, respectively.

Within this study, we comparatively investigated the effects of different thermal cascading strategies on the behavior of a $LaNi_5$-based multi-reactor metal hydride system. To this end, we evaluated equilibrium pressure distributions, energy–exergy performance, and thermo-flow characteristics under increasing-temperature cascading, decreasing-temperature cascading, and isothermal operating conditions. Accordingly, the study provides a comprehensive thermodynamic assessment demonstrating the decisive influence of temperature distribution strategy on hydrogen transfer behavior, pressure amplification characteristics, and system irreversibilities in multi-reactor metal hydride systems.

The main contributions of this study are summarized as follows:

- Comparative evaluation of increasing, decreasing, and isothermal thermal cascading strategies in a $LaNi_5$-based multi-reactor metal hydride system.
- Integrated analysis of equilibrium pressure behavior, energy performance, exergy characteristics, and thermo-flow responses under identical operating conditions.
- Development of a literature-based comparative benchmarking framework using normalized experimental datasets extracted from previously published studies.
- Identification and isolation of temperature-grading direction as an independent thermodynamic design variable governing equilibrium-pressure ordering and the coupled thermal-exergy response of the multi-reactor system.

2. Materials and Methods

This section presents the thermodynamic and numerical modeling approach for the $LaNi_5$-based multi-reactor metal hydride system. Within the scope of this study, the system configuration was defined, fundamental modeling assumptions were established

for different thermal cascading strategies, and equilibrium pressure behavior was modeled using the Van't Hoff relation. In addition, the governing equations used in the energy and exergy analyses are presented, and the numerical solution methodology adopted to investigate thermo-flow behavior is explained. Furthermore, the thermodynamic coupling mechanism between the reactors is described. To benchmark the developed model, a literature-based reduced benchmarking framework and performance evaluation criteria were employed.

2.1. System Description and Thermodynamic Model

This study modeled the system as a thermally cascaded multi-reactor metal hydride (MH) configuration representing hydrogen storage and hydrogen pressure amplification processes. The operating principle is based on the reversible solid–gas reaction between hydrogen and the metal hydride bed under controlled absorption and desorption conditions. In MH systems, temperature, equilibrium pressure, reaction kinetics, and alloy-specific thermodynamic properties primarily govern reaction behavior [1–3,8].

A $LaNi_5$-based configuration was selected because of its suitable equilibrium pressure range and stable hydrogen absorption/desorption characteristics, making it widely used in metal hydride hydrogen compression applications [1,17,18]. The system consisted of three series-connected reactors operated under three different thermal cascading strategies: increasing temperature cascading (T1 < T2 < T3), decreasing temperature cascading (T1 > T2 > T3), and isothermal conditions (T1 = T2 = T3).

The model assumes series reactor operation, homogeneous temperature distribution within each reactor, mass continuity between reactors, and negligible hydrogen losses. This study evaluated equilibrium pressure behavior as a temperature-dependent function using the Van't Hoff approach with constant alloy thermodynamic parameters. In addition, the inter-reactor thermal load distribution was considered according to temperature level and reaction conditions. These assumptions align with reduced-order thermodynamic modeling approaches commonly adopted for metal hydride reactors [9,25].

In MH systems, the equilibrium pressure is commonly expressed using the Van't Hoff relation [1–3].

$$ln\left(\frac{P_{eq}}{P^o}\right) = \frac{\Delta S_{des}}{R} - \frac{\Delta H_{des}}{RT} = A - \frac{B}{T} \quad (1)$$

$$A = \frac{\Delta S_{des}}{R} \quad (2)$$

$$B = \frac{\Delta H_{des}}{R} \quad (3)$$

Here, P_{eq} represents the equilibrium pressure, T denotes temperature, and A and B correspond to alloy-specific thermodynamic constants. Under desorption conditions, the Van't Hoff approach shows that equilibrium pressure increases with temperature. Consequently, higher temperatures enable hydrogen release from the metal hydride bed at elevated pressures [1,26]. To express temperature explicitly, the Van't Hoff relation can be rearranged as follows:

$$T = \frac{B}{A - ln\left(\frac{P_{eq}}{P^o}\right)} \quad (4)$$

For the multi-reactor configuration, the equilibrium pressure was defined separately for each reactor as a function of temperature:

$$\ln\left(\frac{P_{eq,i}}{P^o}\right) = A - \frac{B}{T_i}; \quad i = 1,2,3 \quad (5)$$

In the baseline scenario, the reactor temperatures for the increasing-temperature cascading strategy were set to 300 K, 320 K, and 340 K, respectively. For the decreasing-temperature cascading strategy, the same temperature levels were applied in reverse order, whereas under isothermal operating conditions, all reactors were operated at 320 K. In the isothermal case, 320 K was selected as the reference operating condition representing the average temperature level of the other two thermal strategies. The selected temperature ranges are consistent with the desorption operating conditions reported in the literature for $LaNi_5$-based metal hydride systems [1,26,27].

In the single-reactor reference system, the total metal hydride amount was 3 kg. In the multi-reactor configuration, the total metal hydride amount was kept constant, and a staged $LaNi_5$ distribution of 1.5 kg, 1.0 kg, and 0.5 kg was assigned to the reactors, respectively. This reactor sequence represented different reaction loads and heat-transfer requirements. Similar design approaches considering different reaction zones and heat transfer requirements in multi-tubular and multi-stage metal hydride systems have also been reported in the literature [8,11,14]. To examine the sensitivity of the thermal results to the assumed metal hydride allocation, two additional mass-distribution cases were evaluated while maintaining the same total inventory of 3 kg: a uniform distribution (1.0–1.0–1.0 kg) and a reverse distribution (0.5–1.0–1.5 kg). The reactor temperatures, thermodynamic parameters, and total heat-input basis were kept unchanged. For this sensitivity check, the stage-wise heat input was allocated in proportion to the metal hydride mass assigned to each reactor.

The model's fundamental thermodynamic parameters were determined from literature data for the $LaNi_5$–H_2 system and assumed to remain constant across all comparative analyses. For the $LaNi_5$–H_2 desorption equilibrium adopted in the present model, the thermodynamic parameters were taken as ΔH_{des} = 31.8 kJ mol^{-1} and ΔS_{des} = 110 J mol^{-1} K^{-1}, consistent with reported thermodynamic data for $LaNi_5$ [4]. Using R = 8.314 J mol^{-1} K^{-1}, the corresponding Van't Hoff constants are A = 13.2307 and B = 3824.87 K, respectively [1,28]. The equilibrium pressure is expressed relative to the standard pressure P^0 = 1 bar. These constants yield equilibrium pressures of approximately 1.62, 3.59, and 7.25 bar at 300, 320, and 340 K, respectively, thereby reproducing the values reported in the study [29,30].

2.2. Energy and Exergy Analysis Methodology

Energy and exergy analyses are fundamental approaches for the thermodynamic evaluation of metal hydride-based hydrogen storage systems [29,30]. In particular, temperature distribution and thermal management strategies in multi-reactor metal hydride systems directly affect energy consumption, exergy destruction, and system irreversibilities [1,7,31]. Therefore, in this study, the energy analysis was based on the first law of thermodynamics, while the exergy analysis followed the second-law approach. This study comparatively investigated the effects of different thermal cascading strategies on system behavior.

For each metal hydride reactor, the energy balance under steady-state open control volume conditions can be expressed as follows:

$$\dot{Q}_i + \dot{m}_{H2,i}\,\Delta H = \dot{E}_{out,i}\dot{E}_{in,i} \quad (6)$$

Here, Q_i represents the heat transfer entering or leaving the reactor, $\dot{m}H_{2,i}$ denotes the hydrogen mass flow rate, and ΔH corresponds to the reaction enthalpy of the metal hydride reaction. In metal hydride systems, absorption is exothermic, whereas desorption is endothermic [1,9].

For completeness, the general lumped reactor energy balance including the thermal-storage term can be expressed as follows:

$$\dot{Q}_{tot,i} = m_{MH,i} \times C_{p,MH} \times \left(\frac{dT_i}{dt}\right) + \dot{m}_{H2,i} \times \Delta H \quad (7)$$

Here, m_{MH} represents the mass of the metal hydride, c_p denotes the specific heat capacity, and dT/dt corresponds to the rate of temperature change. Equation (7) represents the general transient form of the reactor energy balance and is provided to identify the sensible thermal-storage contribution explicitly. However, the comparative calculations reported in the present study correspond to prescribed steady operating points rather than time-resolved reactor transients. Therefore, $dT_i/dt = 0$ was imposed in all calculations used to generate the reported results, and Equation (7) was not integrated in time. The present framework should consequently be interpreted as a steady operating-point/equilibrium-pressure model. Predicting heating and cooling transients requires a time-dependent formulation that includes reaction kinetics, hydrogen inventory evolution, and thermal inertia. The equation indicates that the total energy variation within the system originates not only from the reaction heat but also from sensible heat effects associated with temperature variations. Thermo-flow analyses of metal hydride reactors have likewise shown that temperature distribution directly influences system energy behavior [5,26,32].

For the multi-reactor system, the overall energy balance was expressed as the summation of the contributions from all reactors as follows:

$$\dot{Q}_{system} = \sum_{i=1}^{N} \dot{Q}_{tot,i} \quad (8)$$

Here, N represents the total number of reactors in the system. Using this approach, we evaluated each reactor's energy contribution under different thermal strategies and compared the overall energy distribution across the system.

To evaluate system performance, the energy efficiency was defined as follows:

$$\eta_{en} = \frac{\dot{E}_{useful}}{\dot{E}_{input}} \quad (9)$$

Although energy analysis reveals the system's overall energy conversion performance, it is insufficient on its own to evaluate irreversibilities and useful energy losses [30,33]. Therefore, this study performed a second-law-based exergy analysis and assessed system performance using exergy efficiency. Recent studies have emphasized that metal hydride systems should be evaluated not only by energy efficiency but also by exergy-based performance indicators [7,19,33].

To evaluate the second-law-based performance of the system, the exergy efficiency was defined as follows:

$$\eta_{ex} = \frac{\dot{E}_{x,useful}}{\dot{E}_{x,input}} \quad (10)$$

Here, $E_{x,useful}$ represents the useful exergy output obtained from the system, whereas $E_{x,input}$ denotes the total exergy input supplied to the system. This formulation enables the quantitative evaluation of useful energy conversion performance and irreversibilities occurring throughout the process [19,30].

The general exergy balance for the system can be expressed as follows:

$$\dot{E}_{x,dest} = \dot{E}_{x,in} - \dot{E}_{x,out} \quad (11)$$

Here, $E_{x,dest}$ represents the exergy destruction occurring within the system. Exergy destruction arises as a consequence of system irreversibilities and can be defined as follows:

$$\dot{E}_{x,dest} = T_0 * \dot{S}_{gen} \quad (12)$$

Here, T_0 denotes the ambient temperature, while S_{gen} represents the entropy generation rate. This approach enables the evaluation of the effects of different thermal strategies on system irreversibilities. Energy–exergy analyses reported in the literature have also shown that temperature control strategies decisively influence exergy destruction behavior [7,19,30].

For the multi-reactor system, the total exergy was defined as the summation of the contributions of all reactors as follows:

$$\dot{E}_{x,total} = \sum_{i=1}^{N} \dot{E}_{x,i} \quad (13)$$

In the conducted analyses, the influence of temperature distribution direction on system irreversibilities was evaluated. In this context, increasing and decreasing temperature cascading strategies, together with isothermal operating conditions, were comparatively investigated. Previous studies on multi-stage metal hydride compressors have similarly demonstrated that temperature distribution direction directly affects hydrogen transfer performance and overall system efficiency [17,18,22].

The energy and exergy analyses were employed to evaluate the thermodynamic performance of the multi-reactor system configuration and to comparatively investigate the effects of different thermal strategies on overall system behavior.

2.3. Thermo–Flow Numerical Modeling

Heat transfer and flow behavior during absorption and desorption in metal hydride reactors are fundamental mechanisms governing system performance. In particular, effectively supplying the required heat during desorption and efficiently removing the heat released during absorption are critical for reaction kinetics and hydrogen-transfer performance [9,25]. In the present study, a reduced-order numerical model was employed instead of a full-scale computational fluid dynamics (CFD) solution to investigate thermo-flow behavior [25]. The model was developed to represent the system's dominant heat transfer and flow characteristics.

Heat transfer was modeled by considering the combined effects of conduction and convection mechanisms occurring within the metal hydride bed. The convective heat transfer can be expressed as follows:

$$\dot{Q} = h * A * \left(T_s - T_f\right) \quad (14)$$

Here, h represents the convective heat transfer coefficient, A denotes the heat transfer surface area, T_s corresponds to the reactor surface temperature, and T_f represents the fluid temperature [25,26].

Temperature distributions, velocity fields, and heat flux behavior were obtained numerically. The temperature field was defined according to the selected thermal strategies, while the velocity field was modeled assuming laminar flow. This approach is consistent with the assumptions commonly employed for Low-Reynolds-number conditions in metal hydride reactors [9,25].

The heat flux distribution was calculated according to Fourier's law of heat conduction using the temperature gradients derived from the temperature field as follows:

$$\dot{q} = -k * \nabla T \quad (15)$$

Here, k represents the thermal conductivity coefficient, while ∇T denotes the temperature gradient.

The numerical solution procedure was carried out in MATLAB R2021a, and the nonlinear systems of equations were solved using iterative numerical methods. Solution convergence was achieved based on the criterion that the error tolerance remained below $\varepsilon < 10^{-6}$.

Full-scale three-dimensional Computational Fluid Dynamics (CFD) simulations require high computational cost and time. The reduced-order numerical model used in this study was deliberately selected to quickly, effectively, and accurately analyze the fundamental thermodynamic trends in temperature-distribution direction (increasing/decreasing) and thermal cascading on system performance in multi-reactor systems. This simplified approach provides high computational efficiency in representing the macroscopic behavior of the system [9,25].

The model was developed under the following fundamental assumptions:

- The reported thermodynamic and thermo-flow calculations represent prescribed steady operating points; transient thermal-storage and hydrogen-inventory evolution were not solved in time.
- The fluid was assumed to be incompressible.
- The flow regime was considered laminar.
- The reactors were assumed to possess homogeneous properties.
- Heat transfer was modeled through conduction and convection mechanisms.
- Radiation effects were neglected.

These assumptions are consistent with the approaches commonly adopted in reduced-order thermo-flow models of metal hydride reactors [9,34].

2.4. Multi-Reactor Coupling and Literature-Based Benchmarking Methodology

In the present reduced-order framework, the reactor stages are evaluated as thermodynamically staged operating states rather than as a dynamically resolved metal hydride compressor cycle. Accordingly, P_3/P_1 represents a Van't Hoff-based equilibrium-pressure amplification ratio. It should not be interpreted as an experimentally achieved pressure ratio or as the pressure ratio of a fully simulated compressor cycle.

This study represents the multi-reactor configuration as a thermodynamically staged series arrangement. The equilibrium pressure of each reactor is calculated independently from the Van't Hoff relation at its prescribed temperature. Accordingly, the model evaluates the equilibrium-pressure ordering and the associated thermodynamic tendency for staged operation rather than explicitly solving sequential hydrogen transfer between adjacent reactors. This approach aligns with the fundamental operating principle of multi-stage metal hydride compressor systems and reflects behaviors reported in the literature [1,17,18,22].

Within the scope of this study, three operating configurations were evaluated: increasing-temperature cascading (T1 < T2 < T3), decreasing-temperature cascading (T1 > T2 > T3), and isothermal operation (T1 = T2 = T3). Under these configurations, pressure behavior, energy conversion characteristics, and exergy losses were comparatively analyzed.

For actual hydrogen transfer between adjacent stages, a finite gas-phase pressure difference is required. The corresponding physical condition may be expressed conceptually as follows:

$$P_{source} > P_{receiver} + \Delta P_{loss} \tag{16}$$

where P_{source} and $P_{receiver}$ denote the instantaneous gas-phase pressures of the source and receiving reactors, respectively, and ΔP_{loss} represents pressure losses associated with valves, connecting lines, and flow restrictions. This transfer condition is stated as a physical requirement; these transient gas-phase pressures and pressure losses are not solved explicitly in the present reduced-order model. Under the assumption that no hydrogen loss occurred throughout the system, mass continuity was expressed as follows:

$$\dot{m}_i = \dot{m}_{i+1} \tag{17}$$

The mass-continuity relation is retained only as a no-leakage bookkeeping constraint. It is a necessary but not sufficient condition for inter-reactor hydrogen transfer. Actual sequential transfer additionally depends on reaction kinetics, instantaneous hydrogen inventory, valve operation, piping resistance, and transient gas-phase pressure evolution, which are outside the scope of the present steady operating-point model. This approach allowed direct evaluation of how different temperature distributions affect pressure transition behavior within the system.

To assess the reliability of the proposed reduced-order model, a literature-based benchmarking methodology was adopted. Model performance was evaluated using statistical indicators including the mean absolute error (MAE), root mean square error (RMSE), and coefficient of determination (R^2) [34,35].

$$MAE = \frac{1}{n}\sum_{i=1}^{n} |y_i - \hat{y}_i|, \tag{18}$$

$$RMSE = \sqrt{\frac{1}{n}\sum_{i=1}^{n} (y_i - \hat{y}_i)^2}, \tag{19}$$

$$R^2 = 1 - \frac{\sum_{i=1}^{n}(y_i - \hat{y}_i)^2}{\sum_{i=1}^{n}(y_i - \bar{y})^2}, \tag{20}$$

In these statistical metrics, (y_i) represents the reference values extracted from the literature $\hat{y}_i$, denotes the corresponding model predictions, and $\bar{y}$ represents the mean value of the reference dataset.

Because the experimental and numerical studies reported in the literature were conducted at different system scales, the benchmarking analyses used a normalized comparison approach. Within this framework, the relative deviation between the model outputs and literature data was calculated as follows:

$$Relative\ deviation(\%) = \left| \frac{X_{model} - X_{literature}}{X_{literature}} \right| \times 100 \tag{21}$$

Here, X_{model} represents the model output obtained in the present study, whereas $X_{literature,i}$ denotes the reference value reported in the literature. This approach enables comparison of thermodynamic trends within a physically consistent framework when identical operating conditions are unavailable.

To evaluate the overall thermodynamic performance of the system, a dimensionless exergy–pressure performance index combining exergy efficiency and pressure amplification ratio was defined as follows:

$$\Pi = \eta_{ex} * \left(\frac{P_3}{P_1}\right), \tag{22}$$

The index defined in Equation (22) is introduced solely as a dimensionless comparative performance indicator and should not be interpreted as an additional thermodynamic efficiency or as a fundamental performance law. It simultaneously reflects exergy efficiency and the equilibrium-pressure amplification tendency within the investigated configurations. The unit exponents used in the product represent an unweighted baseline formulation rather than a universal assumption that the two quantities have equal engineering importance. Without application-specific economic, operational, or safety weighting criteria, introducing unequal weights would add another arbitrary assumption. Therefore, Π is used only for comparative performance assessment, while the individual thermal-exergy and equilibrium-pressure metrics remain the primary physical indicators.

3. Results and Discussion

This section comparatively evaluated the behavior of $LaNi_5$-based single-reactor and multi-reactor metal hydride systems under different thermal cascading strategies. Within the scope of the analyses, the thermodynamic behavior, energy and exergy performance, pressure amplification mechanism, and thermo-flow characteristics of the systems were investigated in detail. In addition, the physical consistency of the proposed reduced-order model was assessed through comparative benchmarking analyses using experimental and numerical studies reported in the literature. Accordingly, the influence of temperature distribution direction on multi-reactor metal hydride systems was comprehensively demonstrated from both thermodynamic and physical perspectives.

3.1. Multi-Reactor System Behavior

Inter-reactor temperature distribution is a key design parameter governing equilibrium pressure behavior and hydrogen transfer direction in multi-reactor metal hydride systems. Under desorption conditions, increasing temperature raises the equilibrium pressure according to the Van't Hoff relationship, creating a natural pressure-amplification mechanism in multi-stage systems [1,25]. Previous studies have similarly demonstrated that temperature-controlled multi-stage reactor configurations play a decisive role in determining hydrogen transfer performance [17,18,22]. Accordingly, the effects of a single-reactor reference system (SR) and three different thermal cascading strategies on equilibrium pressure distribution and pressure amplification behavior were comparatively evaluated. Table 1 presents the resulting equilibrium pressure distributions and equilibrium-pressure amplification ratios.

Table 1. Effect of thermal grading direction on equilibrium pressure distribution in single-reactor and three-reactor $LaNi_5$-based metal hydride systems.

Case	Configuration	Thermal Strategy	T_1	T_2	T_3	P_1	P_2	P_3	P_3/P_1
SR	Single reactor	Reference	—	320	—	—	3.59	—	1.00
A	Three reactors	Increasing grading	300	320	340	1.62	3.59	7.25	4.48
B	Three reactors	Decreasing grading	340	320	300	7.25	3.59	1.62	0.22
C	Three reactors	Isothermal	320	320	320	3.59	3.59	3.59	1.00

The results in Table 1 clearly show that the selected thermal strategy directly influences the behavior of the multi-reactor system. In Case A, where increasing temperature cascading was applied, the equilibrium pressure increased progressively from 1.62 bar to 7.25 bar as the reactor temperature increased from 300 K to 340 K, resulting in a gradual pressure amplification throughout the system. Under this configuration, the overall equilibrium-pressure amplification ratio (P_3/P_1) was calculated as 4.48. This trend agrees well with

previous studies reporting that increasing temperature enhances hydrogen desorption pressure in $LaNi_5$-based systems [25,27].

In contrast, under Case B, where decreasing-temperature cascading was employed, a reverse pressure distribution developed along the reactor sequence due to progressive temperature reduction, and the overall equilibrium-pressure amplification ratio decreased to 0.22. This opposing thermodynamic trend indicates that inadequate temperature–pressure matching between consecutive reactors weakens the hydrogen transfer mechanism in multi-reactor configurations. Similar observations have been reported for multi-stage metal hydride compression systems, where the coupling between temperature and equilibrium pressure plays a critical role in determining system performance [1,17,18,22].

For Case C, representing isothermal operating conditions, all reactors were maintained at a constant temperature of 320 K. Consequently, no significant pressure gradient developed across the system, and an equilibrium pressure of approximately 3.59 bar was obtained in all stages. This behavior closely resembles that of the single-reactor reference system (SR), demonstrating that isothermal operation alone is insufficient to establish a multi-stage pressure amplification mechanism.

Overall, the results indicate that increasing temperature cascading (Case A) provides the best pressure-amplification performance in the multi-reactor $LaNi_5$-based metal hydride system. The achieved equilibrium-pressure amplification ratio of 4.48 shows that the thermal distribution strategy is not merely an auxiliary operating condition but a key design parameter governing the equilibrium-pressure amplification potential of the system. These findings also provide the thermodynamic basis for the energy, exergy, and thermo-flow analyses presented in the subsequent sections.

3.2. Energy and Exergy Analysis

Temperature distribution, inter-reactor thermal interactions, and reaction load distribution directly influence the energy and exergy behavior of multi-reactor metal hydride systems [1,7,25]. In particular, in multi-stage configurations, temperature distribution is a key parameter governing hydrogen transfer mechanisms and the conversion of thermal energy into useful work [17,18,22,31]. Therefore, the effects of different thermal cascading strategies on energy conversion, exergy behavior, and pressure amplification performance were comparatively investigated. To ensure a consistent basis for comparison, the total metal hydride inventory was maintained at 3 kg in all cases, such that the observed performance differences could be attributed solely to the applied thermal distribution strategies.

System performance was quantitatively evaluated using total heat input, total thermal exergy, exergy destruction, exergy efficiency, and equilibrium-pressure amplification ratio. In addition, an exergy–pressure performance index ($\eta_{ex} \times P_3/P_1$) was introduced to simultaneously assess thermodynamic quality and useful pressure amplification capability. Previous studies have demonstrated that the performance evaluation of metal hydride systems should not be limited to first-law (energy-based) efficiency alone and that second-law (exergy-based) analyses play a critical role in identifying system irreversibilities and thermodynamic losses [7,19,30].

For the comparative analysis, a common normalized total heat-input basis of 1987.5 kJ was prescribed for all configurations rather than independently recalculating the total heat requirement for each thermal strategy. With the total metal hydride inventory fixed at 3 kg, this corresponds to a common comparison basis of 662.5 kJ kg^{-1} of metal hydride. For the baseline 1.5–1.0–0.5 kg distribution, this basis corresponds to stage-wise heat allocations of 993.75, 662.50, and 331.25 kJ, respectively. Maintaining the same total heat-input basis enables the thermal-grading cases to be compared under an equivalent input condition.

Therefore, the value of 1987.5 kJ should be interpreted as a normalized comparison basis and not as a prediction that all configurations would require exactly the same heat input during a complete transient operating cycle.

The results in Table 2 indicate that although the total energy input remained constant at 1987.5 kJ for all cases, the temperature distribution strategy strongly influenced the conversion of thermal energy into useful work [1,17,31]. In Case A, with increasing temperature cascading, the highest equilibrium-pressure amplification ratio (P_3/P_1 = 4.48) and the highest exergy–pressure performance index (Π = 20.98) was obtained. The controlled temperature increases across the reactors established a progressive thermodynamic driving force that enhanced hydrogen transfer throughout the system. Consistent with findings reported by Lototskyy et al. [1] and Parida et al. [17], this behavior indicates more effective conversion of thermal energy into pressure-amplification work.

Table 2. Comparative energy and exergy performance of single-reactor and three-reactor $LaNi_5$-based systems under different thermal grading strategies.

Case	Thermal Strategy	Total Heat Input (kJ)	Thermal Exergy (kJ)	Exergy Destruction (kJ)	Exergy Efficiency (%)	Equilibrium-Pressure Amplification Ratio (P_3/P_1)	Exergy-Pressure Performance Index
SR	Reference	1987.5	136.64	1850.9	6.88	1.00	6.88
A	Increasing grading	1987.5	93.09	1894.4	4.68	4.48	20.98
B	Decreasing grading	1987.5	170.51	1817.0	8.58	0.22	1.89
C	Isothermal	1987.5	136.64	1850.9	6.88	1.00	6.88

In contrast, under Case B, where decreasing-temperature cascading was implemented, the equilibrium-pressure amplification ratio remained only 0.22 despite the relatively high thermal exergy input and exergy efficiency (8.58%). This opposing thermodynamic trend suggests that system performance cannot be evaluated solely on energy or exergy efficiency. It must also consider the system's ability to convert available energy into useful pressure amplification. A similar behavior was observed under the isothermal Case C scenario, where all reactors operated at the same temperature. Under these conditions, no significant pressure gradient developed throughout the system, and the equilibrium-pressure amplification ratio remained at (P_3/P_1 = 1.00), closely resembling the behavior of the single-reactor reference system (SR). The desorption mechanisms reported by Kumar et al. [26] further support the importance of temperature gradients as a driving force for hydrogen release and pressure development. Accordingly, Case B provides the most favorable exergy performance among the investigated configurations, exhibiting the highest exergy efficiency and the lowest exergy destruction. Case A, in contrast, provides the strongest pressure amplification but does not represent the exergy-optimal configuration. Therefore, exergy performance and pressure-amplification performance should be interpreted as two distinct aspects of system behavior.

Figure 2 presents graphical comparisons of the energy and exergy performance metrics.

Examination of the graphical distributions presented in Figure 2 reveals that, despite the relatively lower exergy efficiency observed in Case A, the high exergy–pressure performance index achieved under this configuration highlights the effectiveness of the increasing temperature cascading strategy in converting thermal energy into useful pressure amplification. Studies conducted by Nguyen and Shabani [7] and Ye et al. [15] have similarly demonstrated that appropriately designed thermal management strategies can effectively reduce thermodynamic irreversibilities and enhance overall system performance. Importantly, the higher combined index of Case A should not be interpreted as indicating higher

exergy efficiency or lower exergy destruction; rather, it primarily reflects the substantially greater pressure-amplification contribution of this configuration.

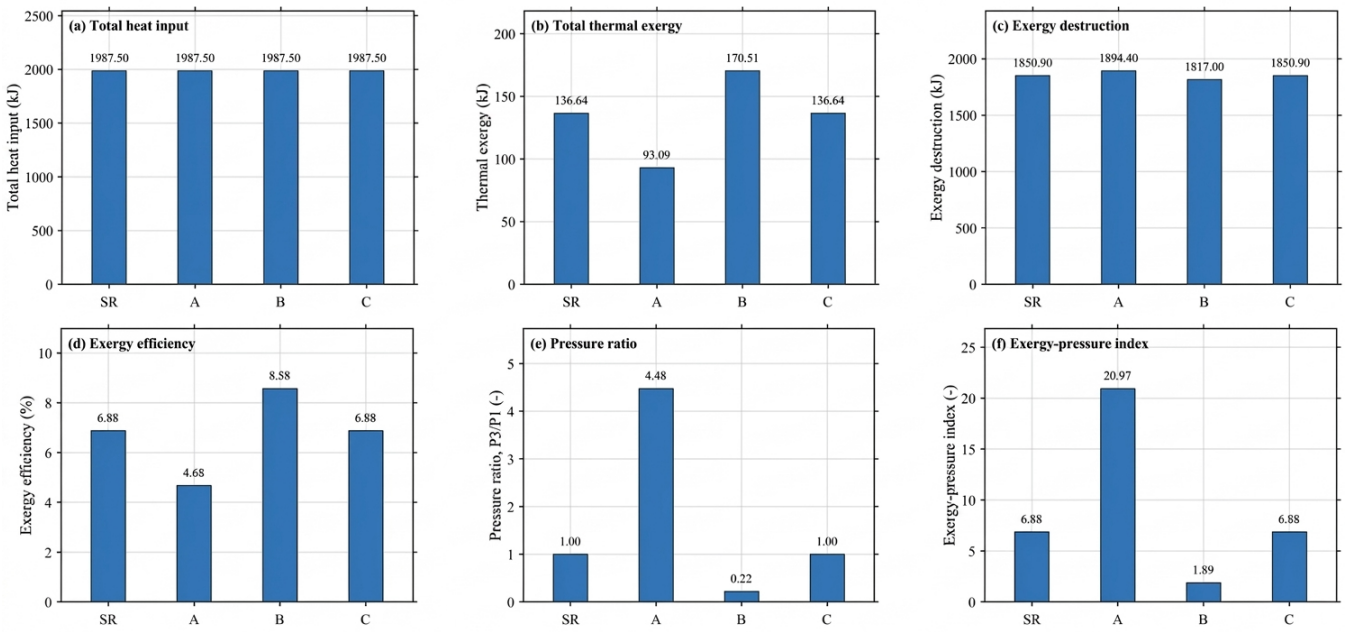


Figure 2. Comparative energy and exergy performance of single-reactor and three-reactor $LaNi_5$-based metal hydride systems under different thermal grading strategies: (**a**) total heat input, (**b**) total thermal exergy, (**c**) exergy destruction, (**d**) exergy efficiency, (**e**) equilibrium-pressure amplification ratio (P_3/P_1), and (**f**) exergy–pressure performance index.

A sensitivity check was performed for the baseline (1.5–1.0–0.5 kg), uniform (1.0–1.0–1.0 kg), and reverse (0.5–1.0–1.5 kg) metal hydride distributions while maintaining the total inventory at 3 kg. Under the common total heat-input basis, the corresponding stage-wise heat allocations were 993.75–662.50–331.25 kJ, 662.50–662.50–662.50 kJ, and 331.25–662.50–993.75 kJ, respectively. For Case A, the calculated exergy efficiency changed from 4.68% for the baseline distribution to 6.63% for the uniform distribution and 8.58% for the reverse distribution. For Case B, the corresponding values were 8.58%, 6.63%, and 4.68%, whereas Case C remained approximately 6.88%. The equilibrium-pressure amplification ratios remained unchanged at 4.48, 0.22, and 1.00 for Cases A, B, and C, respectively, because equilibrium pressure in the present model is determined by temperature through the Van't Hoff relation rather than by the metal hydride mass distribution. Thus, within the present reduced-order framework, mass allocation influences the stage-wise thermal and exergy distribution but does not alter the calculated equilibrium-pressure amplification ratio. Previous studies on multi-tubular metal hydride reactor designs have likewise demonstrated that the interaction between reaction load distribution and thermal management plays a critical role in determining system performance [8,11,14].

Overall, the results indicate that optimum performance in multi-reactor metal hydride systems depends not only on operating temperature but also on the thermal cascading strategy, reactor mass distribution, and thermo-reactive coupling between consecutive reactors. The observed trends are consistent with the current understanding of thermal management and performance optimization in advanced metal hydride systems reported in the recent literature [31].

3.3. Numerical Thermo-Flow Analysis

Thermo-flow behavior is a key mechanism governing the overall performance of metal hydride-based systems because of the strong coupling between temperature distribution,

heat flux, and flow fields [5,9,26]. In multi-reactor configurations, the direction of thermal cascading directly influences equilibrium pressure, reaction kinetics, and heat transfer characteristics [1,15,31]. Accordingly, the temperature fields, velocity distributions, and heat flux characteristics of a single-reactor reference system (SR) and three multi-reactor configurations, namely increasing temperature cascading (Case A), decreasing temperature cascading (Case B), and isothermal operation (Case C), were numerically investigated using a reduced-order thermo-flow model developed in MATLAB R2021a. Heat flux distributions were calculated based on Fourier's law of heat conduction, while the velocity fields were modeled under laminar flow conditions representative of low Reynolds number regimes [28,29].

The numerical results in Figure 3 show that, in the single-reactor reference system (SR), temperature and the associated heat flux decrease continuously and unidirectionally along the reactor length. This behavior is consistent with conventional single-reactor simulations reported in the literature [5,9,26].

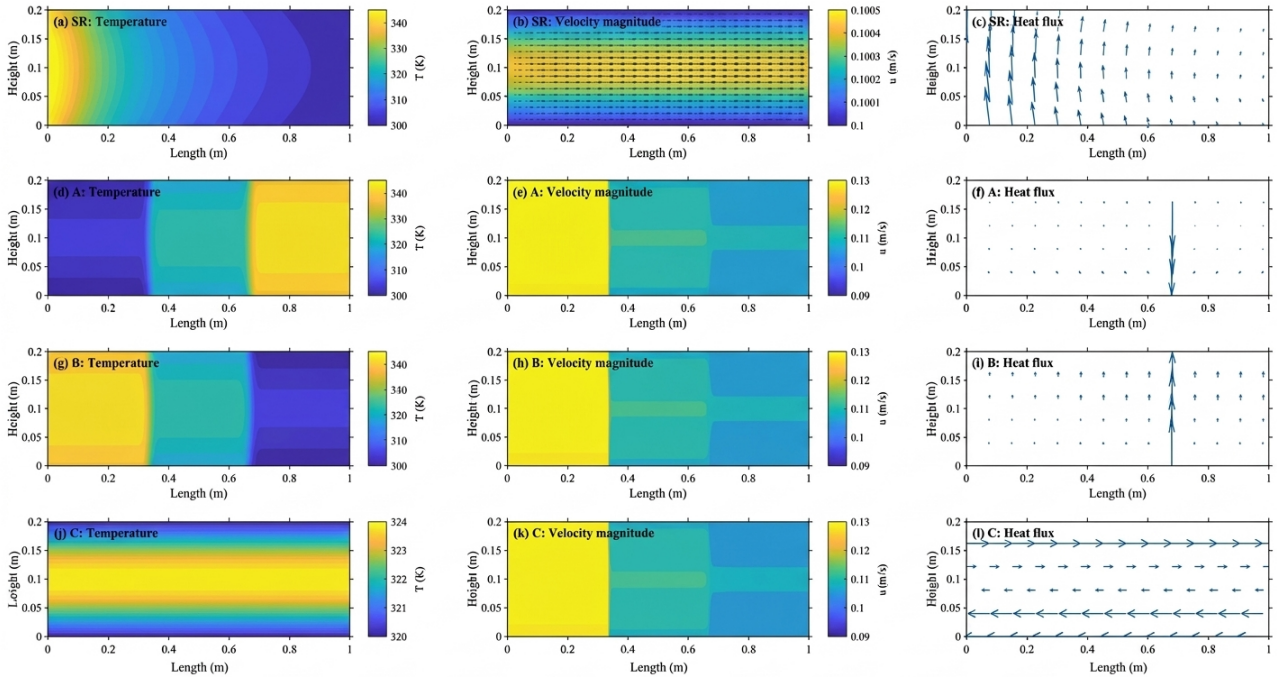


Figure 3. Numerical thermo-flow comparison of $LaNi_5$-based MH systems under different thermal grading strategies: (**a**) temperature distribution, (**b**) velocity magnitude, (**c**) heat-flux vectors for the single-reactor reference (SR); (**d**) Temperature distribution, (**e**) velocity magnitude fields, and (**f**) heat flux vectors for increasing thermal grading (Case A); (**g**) temperature distribution, (**h**) velocity magnitude, and (**i**) heat-flux vectors for decreasing thermal grading (Case B); and (**j**) temperature distribution, (**k**) velocity magnitude, and (**l**) heat-flux vectors for isothermal operation (Case C).

For Case A, where increasing temperature cascading was implemented, the controlled temperature rise across successive reactors produced pronounced temperature gradients and directional heat-flux vectors. As a result, the system developed a more organized thermo-flow structure under the imposed temperature distribution. Previous studies have similarly reported that controlled thermal gradients enhance reaction kinetics and improve hydrogen transport performance by sustaining favorable thermodynamic driving forces [11,15,17,18,22].

In contrast, under Case B, the progressive decrease in temperature along the reactor sequence reversed the heat flux direction and weakened the thermo-flow driving force between reactors. This behavior resulted in less favorable flow-field and thermo-flow characteristics within the reduced-order representation. Similar observations have been

reported in the three-dimensional multiphysics simulations of Bao et al. [25], which demonstrated the significant influence of temperature-gradient direction on the thermo-flow behavior of metal hydride systems.

Under isothermal operating conditions (Case C), no significant temperature gradient developed between reactors, resulting in limited heat-flux distributions and only minor variations in the flow field. As Shafiee [28] notes, the absence of thermal gradients reduces the thermodynamic driving force governing hydrogen transfer, thereby limiting the advantages of multi-stage configurations. Comparable findings have also been reported in previous experimental and numerical investigations of metal hydride systems [14,32,36].

Overall, the thermo-flow analyses provide a physical interpretation of the energy, exergy, and equilibrium-pressure amplification ratio (P_3/P_1) results presented in the preceding sections. The directional heat-flux patterns and relatively stable flow structures observed under increasing-temperature cascading (Case A) help explain the superior pressure-amplification performance achieved under this configuration. These findings suggest that the thermal cascading strategy is a critical design parameter influencing both the thermodynamic performance and operational stability of multi-reactor metal hydride systems [31].

3.4. Model Evaluation and System Comparison

In this section, the performance of the proposed multi-reactor metal hydride system model was comparatively evaluated, and benchmarking analyses were conducted using experimental studies reported in the literature. The physical consistency of the model was investigated in terms of thermodynamic behavior, hydrogen transfer tendencies, thermo-flow transition mechanisms, and system-level performance parameters. In addition, the effects of different thermal cascading strategies on system behavior were comparatively assessed, and the capability of the proposed reduced-order model to represent the behavior of multi-stage metal hydride systems reported in the literature was analyzed.

3.4.1. Literature-Based Benchmarking Using Normalized Experimental Datasets

A literature-based benchmarking assessment was performed using experimental datasets reported in previous studies on metal hydride hydrogen storage and multi-stage hydrogen compression systems. This procedure does not constitute direct experimental validation of the present reactor configuration. Rather, the published datasets were used as external benchmarks to assess whether the reduced-order model reproduces comparable macroscopic thermodynamic and transport trends after normalization. The datasets presented by Kumar et al. [26], Arslan et al. [27], Jana et al. [8], and Parida et al. [17] were used as reference sources to evaluate equilibrium pressure behavior, PCT characteristics, hydrogen release kinetics, thermo-flow behavior, and system-level performance. Numerical data reported in the literature were extracted from the corresponding figures using the WebPlotDigitizer software.

Since the reference studies were conducted using different reactor scales, metal hydride inventories, and hydrogen transfer capacities, the experimental datasets were normalized and scaled according to the capacity of the present $LaNi_5$-based model. In particular, the thermal-energy data were normalized to the common comparison basis adopted for the present 3 kg model. The primary objective of this methodology was not to reproduce the experimental systems directly, but rather to compare macroscopic system behavior, thermodynamic transition characteristics, and the physical dynamics of multi-reactor configurations under a common evaluation framework. The resulting benchmarking dataset is presented in Table 3. Because the reference studies differ from the present model in reactor geometry, metal hydride inventory, operating boundary conditions, hydrogen

capacity, instrumentation, and system scale, the resulting statistical indicators should be interpreted as measures of trend-level correspondence after normalization rather than as measures of predictive accuracy for an identical experimental system. In addition, numerical values digitized from published figures may contain extraction uncertainty. These limitations mean that the present benchmarking exercise cannot substitute for direct experimental validation under matched operating conditions.

Table 3. Comprehensive reduced experimental–literature benchmarking dataset for SR–A–B–C configurations.

Benchmarking Category	Benchmarking Metric	Literature Source	Literature/ Reduced Value	SR	A	B	C	Unit
Thermodynamic	Equilibrium pressure	Kumar et al.	3.59	3.59	7.25	1.62	3.59	bar
Thermodynamic	Equilibrium-Pressure amplification ratio	Parida et al.	4.70	1.00	4.48	0.22	1.00	–
Thermodynamic	PCT desorption pressure range	Kumar et al.	0.048–1.218	0.05–0.80	0.05–1.12	0.05–0.39	0.05–0.78	MPa
Thermodynamic	Van't Hoff desorption trend	Kumar et al.	linear positive trend	moderate	strong	inverse	neutral	–
Kinetic	Maximum H_2 release	Arslan et al.	330.86	287.1	331.0	205.0	300.0	L
Kinetic	H_2 release kinetic trend	Jana et al.	rapid asymptotic rise	moderate	strong	weak	moderate	–
Pressure dynamics	Final reactor pressure	Arslan et al.	2.90	3.59	7.25	1.62	3.59	bar
Pressure dynamics	Pressure decay trend	Arslan et al.	exponential decay	moderate	stabilized staged	unstable reverse	stable neutral	–
Flow dynamics	Initial flow rate	Arslan et al.	0.166	0.142	0.165	0.081	0.128	L/s
Flow dynamics	Final flow rate	Arslan et al.	0.007	0.012	0.008	0.031	0.015	L/s
System-level	Exergy efficiency	Parida et al.	4.90	6.88	4.68	8.58	6.88	%
System-level	Maximum operating temperature	Parida et al.	364.35	320	340	340	320	K
System-level	Scaled thermal energy input	Parida et al. (scaled)	5518.69	1987.5	1987.5	1987.5	1987.5	kJ

Note: Qualitative trend descriptors such as "strong", "moderate", "weak", "inverse", "neutral", "stabilized staged", and "unstable reverse" were assigned based on the relative behavior observed in the corresponding literature datasets and the normalized model outputs. These descriptors are intended to provide a comparative interpretation of system trends rather than quantitative performance metrics.

Examination of Table 3 indicates that Case A, corresponding to increasing temperature cascading, exhibits the closest agreement with the multi-stage metal hydride hydrogen compression (MHHC) behavior reported in the literature. In particular, the overall equilibrium-pressure amplification ratio of 4.48 obtained for Case A compares favorably with the experimental reference value of 4.70 reported by Parida et al. [17], suggesting that the proposed thermal strategy successfully captures the fundamental pressure amplification mechanism of multi-stage systems.

From a kinetic and flow-dynamics perspective, the maximum hydrogen release volume obtained in Case A (331.0 L) and the corresponding flow decay behavior show trends comparable to the experimental observations reported by Arslan et al. [27]. Likewise, the asymptotic hydrogen transfer trends presented by Jana et al. [8] indicate that the proposed model is capable of reproducing the dominant kinetic characteristics observed within the

reactor system. In contrast, the reverse thermodynamic direction represented by Case B results in a noticeable deviation from the metal hydride hydrogen compression (MHHC) trends reported in the literature.

The differences observed in the system-level energy performance are primarily associated with the reduced-order modeling approach adopted in the present study. Thermal inertia effects of auxiliary equipment, pressure losses within piping systems, and uncontrolled environmental heat losses reported in experimental systems such as those of Parida et al. [17] were not explicitly included in the model formulation. Nevertheless, the proposed numerical framework was able to reproduce the principal thermodynamic trends, kinetic behavior, and the effects of thermal management strategies with a level of consistency that is appropriate for comparative thermodynamic assessment.

3.4.2. Comparative Statistical Assessment of Literature-Based Benchmarking

A comparative statistical assessment was conducted to evaluate the capability of the proposed reduced-order model to reproduce the dominant thermodynamic and transport trends reported in the literature. The assessment simultaneously considered thermodynamic equilibrium behavior, hydrogen transfer kinetics, pressure amplification mechanisms, flow characteristics, and system-level energy performance. The statistical evaluation included the calculation of normalized mean absolute error (Normalized MAE), normalized root mean square error (Normalized RMSE), the coefficient of determination (R^2), and mean relative deviation (MRD). Reference datasets were established using the thermodynamic PCT and Van't Hoff data reported by Kumar et al. [26], the pressure, flow-rate, and hydrogen release characteristics presented by Arslan et al. [27], the kinetic hydrogen transfer trends reported by Jana et al. [8], and the performance data of multi-stage metal hydride hydrogen compression systems reported by Parida et al. [17].

Because the reference studies were conducted at different system scales, the experimental datasets were normalized and scaled according to the capacity of the present $LaNi_5$-based system. All assessment procedures were subsequently performed using this unified dataset. The statistical results revealed a high log-space coefficient of determination ($R^2 = 0.978$) for the increasing-temperature configuration, indicating that the model closely reproduces the overall variation and trend of the normalized literature data. However, the mean relative deviation (MRD) was approximately 18.4%, indicating that noticeable differences remain in the magnitude of individual predicted values. These two metrics describe different aspects of model performance: R^2 characterizes trend correlation, whereas MRD quantifies the average magnitude of relative deviation. Therefore, the results indicate strong trend-level correspondence but a moderate level of quantitative deviation. This deviation can be attributed to uncontrolled heat losses through reactor walls, thermal inertia effects associated with auxiliary components such as valves and connecting pipes, and measurement uncertainties inherent to experimental systems. Consequently, the reduced-order approach adopted in the present study, which neglects these dynamic losses and evaluates the system under steady-state conditions, provides a reasonable framework for assessing the theoretical performance limits of multi-reactor metal hydride configurations [17,26,27]. The complete statistical benchmarking results are summarized in Table 4.

Table 4. Statistical benchmarking summary of SR–A–B–C configurations.

Case	Thermal Strategy	Normalized MAE	Normalized RMSE	Log-Space (R^2)	Mean Relative Deviation (%)
SR	Single-reactor reference	0.421	0.506	0.913	42.1
A	Increasing thermal grading	0.184	0.297	0.978	18.4

Table 4. *Cont.*

Case	Thermal Strategy	Normalized MAE	Normalized RMSE	Log-Space (R^2)	Mean Relative Deviation (%)
B	Decreasing thermal grading	0.611	0.702	0.691	61.1
C	Isothermal operation	0.447	0.531	0.902	44.7

Table 4 shows that, among the investigated configurations, Case A most closely matches the normalized literature benchmarks. The normalized MAE and RMSE values of 0.184 and 0.297, together with R^2 = 0.978, indicate that Case A provides the closest trend-level correspondence among the investigated configurations. However, the MRD of 18.4% demonstrates that this correspondence should not be interpreted as high absolute predictive accuracy. In particular, the agreement observed with the staged pressure amplification behavior reported by Parida et al. [17] indicates that the model provides a physically consistent representation of the thermodynamic driving-force mechanism underlying multi-stage hydrogen compression systems.

In contrast, Case B, representing decreasing temperature cascading, exhibited substantially larger statistical errors. The normalized MAE and RMSE values increased to 0.611 and 0.702, respectively, while the mean relative deviation reached 61.1%. These results indicate that the reverse temperature distribution strategy deviates considerably from experimentally observed multi-stage metal hydride system behavior. Moreover, the reduction in the R^2 value to 0.691 suggests that the reverse thermal gradient configuration generates system responses that are less consistent with the trends reported in the literature.

For the single-reactor reference system (SR) and the isothermal operating condition (Case C), similar assessment results were obtained. In both cases, the error metrics remained at moderate levels, with correlation coefficients of approximately $R^2 \approx 0.90$. Although these configurations adequately reproduce the general thermodynamic tendencies of the system, they are less capable of representing the staged pressure amplification behavior and dynamic transfer characteristics expected from multi-reactor configurations.

Overall, the assessment results indicate that increasing temperature cascading provides the most favorable thermodynamic transition behavior among the investigated operating strategies. The relatively low error metrics and high correlation coefficients demonstrate that the proposed reduced-order model can serve as a useful engineering tool for the comparative assessment and preliminary optimization of multi-reactor metal hydride systems.

4. Conclusions

This study comparatively investigated the effects of different thermal cascading strategies on the thermodynamic behavior of $LaNi_5$-based single-reactor and multi-reactor metal hydride hydrogen storage systems in terms of energy, exergy, pressure transition, and thermo-flow characteristics. Based on the analyses conducted under increasing temperature cascading, decreasing temperature cascading, and isothermal operating conditions, it was demonstrated that temperature distribution direction constitutes a decisive design parameter governing overall system performance.

Main Findings: Under increasing-temperature cascading conditions (300–320–340 K), the system achieved a gradual equilibrium pressure increase, with calculated pressure levels of approximately 1.62 bar, 3.59 bar, and 7.25 bar, respectively. Consequently, the investigated thermal grading yielded a Van't Hoff-based equilibrium-pressure amplification ratio of approximately P_3/P_1 = 4.48.

Under decreasing temperature cascading conditions (340–320–300 K), a reverse pressure behavior developed along the reactors, and the equilibrium-pressure amplification ratio remained at approximately 0.22. This result shows that the direction of the temperature distribution directly influences equilibrium-pressure ordering and the associated thermodynamic driving tendency.

Under isothermal operating conditions (320 K), similar equilibrium pressures were obtained in all reactors, and no significant multi-stage pressure amplification behavior was observed. This finding indicates that not only the temperature level but also the temperature gradient is critical for overall system performance.

Energy analyses demonstrated that increasing temperature direction significantly enhanced hydrogen desorption capacity and thermodynamic driving force. Accordingly, the imposed temperature distribution yielded a stronger thermodynamic driving tendency.

The exergy analysis showed that decreasing temperature grading (Case B) provided the highest exergy efficiency (8.58%) and the lowest exergy destruction (1817.0 kJ), whereas increasing temperature grading (Case A) exhibited a lower exergy efficiency (4.68%) and a higher exergy destruction (1894.4 kJ). Therefore, Case B was the most favorable configuration from the exergy perspective, while the main advantage of Case A was its substantially greater pressure-amplification capability.

Thermo-flow analyses showed that controlled temperature gradients produced more organized temperature fields, directional heat-flux distributions, and more stable flow behavior. In particular, more regular thermo-reactive transition mechanisms were observed under increasing temperature direction.

The literature-based comparison yielded (R^2 = 0.978) and an MRD of 18.4% for the increasing-temperature configuration, indicating strong trend-level correspondence but moderate quantitative deviation. These results should not be interpreted as direct experimental validation of the present system.

The obtained findings indicate that the performance of multi-reactor metal hydride systems depends not only on temperature level but also strongly on temperature distribution direction and thermo-reactive interactions between reactors. Therefore, the thermal distribution strategy should be considered a fundamental optimization parameter in system design.

Future Perspectives: Future studies should focus on experimentally validating the proposed model, incorporating advanced thermo-flow solution approaches, and applying the methodology to different metal hydride alloys. In addition, integrating artificial intelligence and data-driven optimization techniques into temperature-control strategies is a promising research direction for improving the performance and operational reliability of multi-reactor metal hydride systems.

Funding: This research received no external funding.

Institutional Review Board Statement: Not applicable.

Informed Consent Statement: Not applicable.

Data Availability Statement: The data supporting the findings of this study are included within the article. No publicly archived dataset was generated during the study. The literature-based benchmarking data were derived from previously published studies cited in the manuscript and were normalized for comparative assessment.

Conflicts of Interest: The author declares no conflicts of interest.

Abbreviations

The following abbreviations are used in this manuscript:

Abbreviation	Definition
MH	Metal hydride
H_2	Hydrogen
$LaNi_5$	Lanthanum nickel hydride-forming alloy
SR	Single reactor
PCT	Pressure–composition–temperature
PCM	Phase change material
CFD	Computational fluid dynamics
MAE	Mean absolute error
RMSE	Root mean square error
R^2	Coefficient of determination
MRD	Mean relative deviation
MHHC	Metal hydride hydrogen compressor

References

1. Lototskyy, M.; Yartys, V.A.; Pollet, B.G.; Bowman, R.C. Metal hydride hydrogen compressors: A review. *Int. J. Hydrogen Energy* **2014**, *39*, 5818–5851. [CrossRef]
2. Sandrock, G. A panoramic overview of hydrogen storage alloys from a gas reaction point of view. *J. Alloys Compd.* **1999**, *293–295*, 877–888. [CrossRef]
3. Sakintuna, B.; Lamari-Darkrim, F.; Hirscher, M. Metal hydride materials for solid hydrogen storage: A review. *Int. J. Hydrogen Energy* **2007**, *32*, 1121–1140. [CrossRef]
4. Hirscher, M.; Yartys, V.A.; Baricco, M.; von Colbe, J.M.B.; Blanchard, D.; Bowman, R.C.; Broom, D.P.; Buckley, C.E.; Chang, F.; Chen, P.; et al. Materials for hydrogen-based energy storage—Past, recent progress and future outlook. *J. Alloys Compd.* **2020**, *827*, 153548. [CrossRef]
5. Liu, Y.; Ayub, I.; Khan, M.R.; Yang, F.; Wu, Z.; Zhang, Z. Numerical investigation of metal hydride heat storage reactor with two types multiple heat transfer tubes structures. *Energy* **2022**, *253*, 124142. [CrossRef]
6. Li, Q.; Lu, Y.; Luo, Q.; Yang, X.; Yang, Y.; Tan, J.; Dong, Z.; Dang, J.; Li, J.; Chen, Y.; et al. Thermodynamics and kinetics of hydriding and dehydriding reactions in Mg-based hydrogen storage materials. *J. Magnes. Alloys* **2021**, *9*, 1922–1941. [CrossRef]
7. Nguyen, H.Q.; Shabani, B. Thermal management of metal hydride hydrogen storage using phase change materials for standalone solar hydrogen systems: An energy/exergy investigation. *Int. J. Hydrogen Energy* **2022**, *47*, 1735–1751. [CrossRef]
8. Jana, S.; Muthukumar, P. Design, development and hydrogen storage performance testing of a tube bundle metal hydride reactor. *J. Energy Storage* **2023**, *63*, 106936. [CrossRef]
9. Askri, F. Prediction of transient heat and mass transfer in a closed metal–hydrogen reactor. *Int. J. Hydrogen Energy* **2004**, *29*, 195–208. [CrossRef]
10. Raju, M.; Kumar, S. Optimization of heat exchanger designs in metal hydride based hydrogen storage systems. *Int. J. Hydrogen Energy* **2012**, *37*, 2767–2778. [CrossRef]
11. Pandey, V.; Krishna, K.V.; Maiya, M.P. Numerical modelling and heat transfer optimization of large-scale multi-tubular metal hydride reactors. *Int. J. Hydrogen Energy* **2023**, *48*, 16020–16036. [CrossRef]
12. Bulut, H.; Demirtaş, Y.; Beyazit, N.I. Investigation of the effect of different materials on thermal performance of earth-air heat exchanger (EAHX). *J. Fac. Eng. Archit. Gazi Univ.* **2018**, *33*, 1505–1516.
13. Parashar, S.; Muthukumar, P.; Kumar, E.A.; Soti, A.K. Experimental study on multi tube metal hydride reactor for medium temperature hydrogen and thermochemical energy storage applications. *Renew. Energy* **2025**, *242*, 122350. [CrossRef]
14. Parashar, S.; Muthukumar, P.; Soti, A.K. Design optimization and numerical investigation of multi tube metal hydride reactor for large capacity hydrogen storage application. *Therm. Sci. Eng. Prog.* **2024**, *49*, 102468. [CrossRef]
15. Ye, Y.; Zhang, Z.; Liu, J.; Yan, K.; Wang, W.; Cheng, H. Experiment and simulation study on transfer phenomena and performance optimization of MgH_2-based hydrogen storage reactors. *Int. J. Hydrogen Energy* **2024**, *86*, 649–661. [CrossRef]
16. Atalmis, G.; Toros, S.; Timurkutluk, B.; Kaplan, Y. 2D-axisymmetrical modeling and experimental study of hydrogen absorption in copper coated metal hydride. *Int. J. Hydrogen Energy* **2023**, *48*, 38400–38411. [CrossRef]
17. Parida, A.; Kumar, A.; Muthukumar, P.; Dalal, A.; Kumar, S.K.A. Experimental study and performance evaluation of a large-scale multistage metal hydride-based hydrogen compressor. *Appl. Energy* **2025**, *390*, 125798. [CrossRef]
18. Parida, A.; Muthukumar, P.; Dalal, A. Numerical study of a three-stage metal hydride hydrogen compressor considering alloy bed deformation. *Energy Sources Part A Recovery Util. Environ. Eff.* **2024**, *46*, 12414–12434. [CrossRef]

19. Beyazit, N.İ. Energy and exergy analysis of a metal hydride-based hydrogen storage system: A parametric approach. *Dicle Üniversitesi Mühendislik Fakültesi Mühendislik Derg.* **2025**, *16*, 1015–1031. [CrossRef]
20. Beyazit, N.İ. Comparative study of hydrogen storage and metal hydride systems: Future energy storage solutions. *Processes* **2025**, *13*, 1506. [CrossRef]
21. Beyazit, N.İ. Journey to a sustainable future: The importance of renewable hydrogen in industrial and domestic applications. *Int. J. Hydrogen Energy* **2024**, *99*, 836–851. [CrossRef]
22. Parida, A.; Muthukumar, P.; Dalal, A. Experimental evaluation of hydrogen transfer dynamics in a multistage metal hydride hydrogen compressor. *J. Alloys Compd.* **2025**, *1045*, 184482. [CrossRef]
23. Milojević, S.; Savić, S.; Ašonja, A.; Miladinović, S.; Stojanović, B. Electric Propulsion Systems of Autonomous Hydrogen Fuel Cell Buses. *Adv. Eng. Lett.* **2026**, *5*, 51–58. [CrossRef]
24. Kaplan, Y.; Veziroğlu, T.N. Mathematical modelling of hydrogen storage in a $LaNi_5$ hydride bed. *Int. J. Energy Res.* **2003**, *27*, 1027–1038. [CrossRef]
25. Bao, Z.; Wu, Z.; Nyamsi, S.N.; Yang, F.; Zhang, Z. Three-dimensional modeling and sensitivity analysis of multi-tubular metal hydride reactors. *Appl. Therm. Eng.* **2013**, *52*, 97–108. [CrossRef]
26. Kumar, S.; Kojima, Y.; Dey, G.K. Thermodynamics and kinetics of hydrogen absorption–desorption of highly crystalline $LaNi_5$. *J. Therm. Anal. Calorim.* **2018**, *134*, 889–894. [CrossRef]
27. Arslan, B.; İlbaş, M.; Çelik, S. Experimental analysis of hydrogen storage performance of a $LaNi_5$–H_2 reactor with phase change materials. *Int. J. Hydrogen Energy* **2023**, *48*, 6010–6022. [CrossRef]
28. Shafiee, S. Operational principles and effect of operating parameters on performance of metal hydride heat pumps. *Int. J. Refrig.* **2020**, *120*, 22–30. [CrossRef]
29. Çengel, Y.A.; Boles, M.A. *Thermodynamics: An Engineering Approach*, 4th ed.; McGraw-Hill: New York, NY, USA, 2002.
30. Bejan, A. *Advanced Engineering Thermodynamics*; John Wiley & Sons: Hoboken, NJ, USA, 2016. [CrossRef]
31. Prakash, K.S.; Sharma, V.K. Recent developments on metal hydride hydrogen compressors—A comprehensive review. *J. Alloys Compd.* **2025**, *1037*, 182505. [CrossRef]
32. Ran, R.; Wang, J.; Yang, F.; Imin, R. Fast design and numerical simulation of a metal hydride reactor embedded in a conventional shell-and-tube heat exchanger. *Energies* **2024**, *17*, 712. [CrossRef]
33. Dincer, I.; Rosen, M.A. *Exergy: Energy, Environment and Sustainable Development*; Newnes: Oxford, UK, 2012.
34. Breiman, L. Random forests. *Mach. Learn.* **2001**, *45*, 5–32. [CrossRef]
35. Hastie, T.; Tibshirani, R.; Friedman, J. *The Elements of Statistical Learning*; Springer: New York, NY, USA, 2009. [CrossRef]
36. Parashar, S.; Muthukumar, P.; Soti, A.K. Experimental study on embedded cooling tube type metal hydride reactor for hydrogen storage, space heating and cooling applications. *Therm. Sci. Eng. Prog.* **2024**, *58*, 103183. [CrossRef]

Disclaimer/Publisher's Note: The statements, opinions and data contained in all publications are solely those of the individual author(s) and contributor(s) and not of MDPI and/or the editor(s). MDPI and/or the editor(s) disclaim responsibility for any injury to people or property resulting from any ideas, methods, instructions or products referred to in the content.